Electronic structure of the thallium-induced 2×1 reconstruction on Si(001)

P. E. J. Eriksson,[1] Kazuyuki Sakamoto,[2] and R. I. G. Uhrberg[1]
[1]*Department of Physics, Chemistry and Biology, Linköping University, S-581 83 Linköping, Sweden*
[2]*Graduate School of Advanced Integration Science, Chiba University, Chiba 263-8522, Japan*
(Received 22 February 2010; published 17 May 2010)

With a Tl coverage of one monolayer, a 2×1 reconstruction is formed on the Si(001) surface at room temperature. In this study, low-temperature angle-resolved photoelectron spectroscopy (ARPES) data reveal four surface state bands associated with this Tl induced reconstruction. Calculated surface state dispersions, obtained using the "pedestal+valley-bridge" model, are found to be similar to those obtained using ARPES. Inclusion of spin-orbit coupling in the calculations is found to be important to arrive at these results. A known effect of the strong spin-orbit coupling is the reluctance of the Tl $6s^2$ electrons to participate in the bonding, i.e., the inert pair effect. In the calculations, inclusion of spin-orbit coupling results in a ~5 eV downshift of the Tl $6s^2$ electrons.

DOI: 10.1103/PhysRevB.81.205422 PACS number(s): 73.20.At, 71.15.−m, 79.60.Dp

I. INTRODUCTION

The atomic and electronic structures of reconstructions induced by adsorption of group-III metals on Si surfaces have attracted a lot of attention through the years. These studies have mainly been focused on Al, Ga, and In. Only recently, the attention has turned to Tl, the heaviest of the group III metals. Tl exhibits the peculiar inert pair effect, i.e., the $6s^2$ electrons tend to not participate in the bonding due to the strong spin-orbit coupling.[1] As a consequence, Tl can exhibit a 1+ valence state, contrary to the other group-III metals. By varying the temperature conditions, Tl was found to exhibit both the 1+ and the 3+ valence states in a study of the Si(111):Tl surface.[2] Later, the valence state was found to be independent of coverage, as no evidence of the 3+ valence state was found for Tl coverages up to 1 monolayer (ML) in a core-level study of the same surface.[3]

At sub-ML Tl coverages, the Si(001) surface exhibits a series of 2×2 reconstructions while a 2×1 reconstruction is formed with 1 ML coverage.[4] Of the group-III metals, Tl is the only one that gives rise to a 1 ML 2×1 reconstruction. Total energy calculations and scanning tunneling microscopy (STM) have suggested that the "pedestal+valley-bridge" model is the likely atomic structure of this surface.[4] This model is the same as the so called "double-layer model"[5] that has been found to be favorable for the monovalent alkali metals on Si(001).[6] A similar 2×1 structure has been found on the Ge(001):Tl surface at 1 ML coverage.[7]

Both these 1 ML Ge(001):Tl and Si(001):Tl surfaces undergo phase transitions at low temperatures. The Ge(001):Tl surface develops a large $c(12\times14)$ periodicity as observed in STM.[8] The Si(001):Tl surface on the other hand, has been shown, using STM, to transform into a $(6,1)\times(0,6)$ periodicity.[9] This is not observed in low-energy electron diffraction (LEED). The diffraction pattern resembles that of a $c(4\times6)$ periodicity.[10]

The variable valence state and the low-temperature phase transitions make the Tl induced reconstructions interesting. Further, Si(001):Tl has a possibility to show interesting spin splitting that originates from the Rashba effect[11] in similarity to Si(111):Tl (Ref. 12) and Si(111):Bi.[13,14] In this paper, the surface electronic structure of the Si(001):Tl 2×1 surface is investigated using angle-resolved photoelectron spectroscopy (ARPES) at low temperature and theoretical calculations.

II. DETAILS

All experimental work was conducted at beamline 33 at the MAX-I storage ring at the MAX-lab synchrotron radiation facility in Lund, Sweden. In the photoemission measurements, a hemispherical electron analyzer (ARUPS-10, VG) mounted on a goniometer was used. The energy resolution was about 50 meV and the angular resolution was ±2°. The Si(001) sample (*n*-type phosphorous, 2 Ω cm) was thoroughly outgassed and, as a last step, annealed at 1500 K. Thallium was deposited from a Ta foil tube onto the sample at room temperature (RT). The quality of the resulting surface reconstructions was assessed by inspection of LEED patterns. During measurements, the base pressure in the chamber was below 4×10^{-11} torr and, through the use of liquid N_2, a sample temperature of about 100 K was attained. The Fermi level of a Ta foil in electrical contact with the sample was used as reference in the ARPES data.

The theoretical results were obtained by density-functional-theory calculations in the generalized gradient approximation,[15] using the full-potential (linearized) augmented plane-wave+local orbitals method within the WIEN2K code.[16] The atomic slabs that were used for the structure relaxation consisted of 16 Si layers, had an inversion center in the middle and Tl on both surfaces. The irreducible Brillouin zone was sampled with eight **k** points and the energy cutoff was 147 eV. For the band-structure calculations, an H-terminated slab consisting of 12 Si layers was employed and the energy cutoff was 264 eV. The Tl 5*d* states were treated as valence states in all calculations.

III. RESULTS AND DISCUSSION

The effect of Tl adsorption on the surface periodicity was monitored using LEED. At sub ML coverages, relatively weak 2×2 spots indicated the presence of the low-coverage

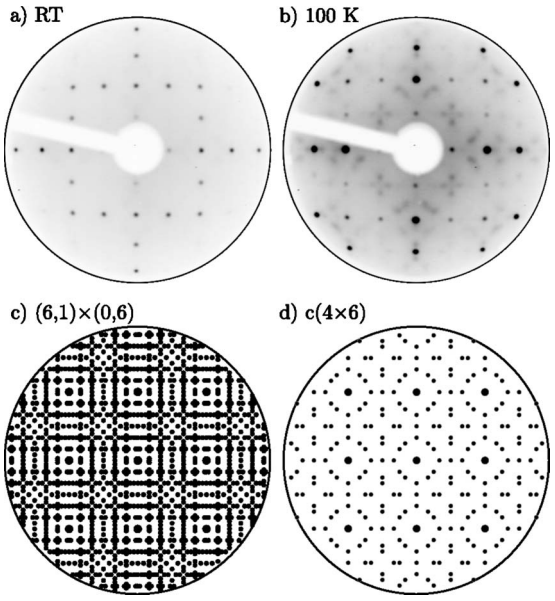

FIG. 1. LEED patterns obtained at (a) RT using 111 eV electrons and (b) at 100 K using 94 eV electrons. (c) and (d) show simulated LEED patterns of two domain $(6,1)\times(0,6)$ and $c(4\times6)$ reconstructions, respectively. In (d), integer order spots are recognized as they are slightly larger. The size of the simulated patterns matches the one in (b).

2×2 surface reconstructions that have been reported on the Si(001):Tl surface.[4] With increasing coverage, the 2×2 spots disappeared and the surface instead showed a sharp 2×1 LEED pattern. Tl adsorption also induced a change in the work function of the sample, from 4.85 eV for the clean Si(001),[17] via 4.21 eV for the 0.5 ML 2×2 phase, to 3.87 eV for the 1 ML 2×1 reconstruction. Such substantial changes in the work function could be the result of the formation of a Tl induced dipole layer on the surface as suggested from the STM study in Ref. 4.

LEED patterns obtained at RT and at 100 K, are shown in Figs. 1(a) and 1(b). Due to monatomic steps on the surface, two orientations of the surface reconstruction exist. Based on inspection of the LEED pattern, these two domains were estimated to cover about 50% of the surface area, each. STM studies have revealed the formation of a $(6,1)\times(0,6)$ surface periodicity at about 120 K.[9] That phase was preserved down to 6 K. A simulated two domain LEED pattern corresponding to the $(6,1)\times(0,6)$ periodicity is shown in Fig. 1(c). This is clearly not what is observed experimentally. Instead, the low-temperature LEED pattern in Fig. 1(b) is very similar to that in Ref. 10 where it was suggested to represent a $c(4\times6)$ surface periodicity. Even though there are many qualitative similarities between the low-temperature LEED pattern and the simulated $c(4\times6)$ pattern in Fig. 1(d), there are also differences. For example, many spots are missing and there is a clear discrepancy in the appearance of, e.g., the four diffraction spots surrounding the $(\frac{1}{2},\frac{1}{2})$ positions. These four spots show $\frac{1}{5}$ distances and other spots can be described by a $c(4\times8)$ periodicity. The LEED pattern appears to be a complicated combination of several different periodicities as it cannot be described by a single unit cell.

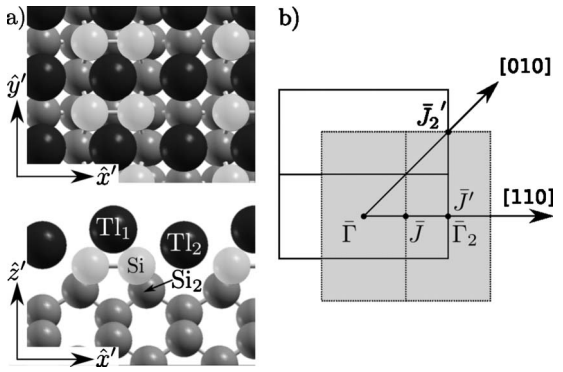

FIG. 2. Geometry of the 2×1 Si(001):Tl surface. (a) shows the atomic structure of the pedestal+valley-bridge model from Ref. 4. The images were prepared using the XCRYSDEN program (Ref. 18). The overlapping SBZs of the two domains are shown in (b) along with the directions investigated with ARPES and surface band-structure calculations.

The surface band structure of the Si(001):Tl 2×1 surface was measured using ARPES at the same temperatures as was used in the LEED study. Apart from the increased thermal broadening at RT, compared to 100 K, no discernible difference in the surface band structure could be detected. Thus, the reversible phase transition, as observed in LEED, does not appear to affect the surface band structure. The surface structure, with two Tl atoms in the 2×1 unit cell, has been attributed to the pedestal+valley-bridge model,[4] as illustrated in Fig. 2(a). Above the transition temperature, e.g., at RT, Tl_2 is rapidly hopping between two local energy minima at different x' positions in the trough between the Si dimer rows.[9] At lower temperature, the hopping frequency decreases. While the surface band structure remains unaffected, long-range order develops and gives rise to a periodicity which is characterized by a larger unit cell as observed in LEED and STM. An analogous behavior is found on, e.g., the clean Si(001) surface. There, the surface dimers are rapidly flipping between two tilt directions. At RT, this gives rise to a 2×1 surface periodicity as observed in LEED and STM. At low temperature, the clean Si(001) surface assumes a $c(4\times2)$ periodicity. The surface band structure, on the other hand, reflects the $c(4\times2)$ periodicity also at RT.

Figures 3(a) and 3(b) show color maps of features in the low-temperature ARPES data along the [110] and [010] directions, respectively, see Fig. 2(b). Photoemission spectra were acquired at 1° intervals using an incidence angle of 45°. In the figures, the intensity in the color maps represents the curvature in the ARPES data as it was processed using a Savitzky-Golay method.[20] Six identified surface state bands are marked by dotted curves. Four of those, S_1-S_4, are associated with the Tl induced reconstruction. Two, S_d and S_{bb}, are very weak and are believed to be of different origin. S_1 is seen closest to E_F around the $\bar{J}_2'$ and $\bar{J}'(\bar{\Gamma}_2)$ points in the two directions, respectively. Since it is not observed around $\bar{\Gamma}$, it is associated with the vicinity of $\bar{J}'$ in the surface Brillouin zone (SBZ). In the [010] azimuth, Fig. 3(b), S_1 appears to show a downward dispersion, reaching 0.7 eV at $\bar{J}_2'$. There are however discontinuities symmetrically on both sides of

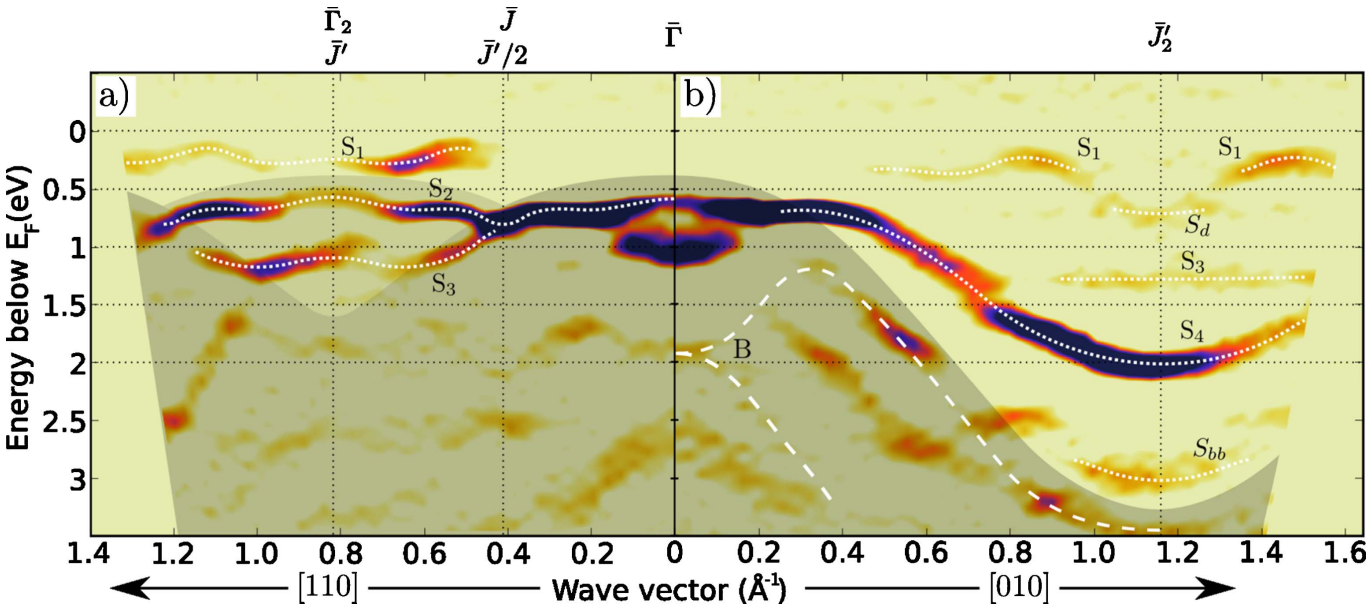

FIG. 3. (Color online) Color map showing features in 21.2 eV ARPES data obtained at 100 K along (a) the [110] direction and (b) the [010] direction. Six identified surface state bands are marked by dotted curves. Four bands associated with the Tl induced reconstruction are labeled S_1-S_4. Those labeled S_d and S_{bb} are believed to be of different origin. In (b), the dashed curves labeled B, indicate the dispersions of direct bulk transitions (Ref. 19). The shaded regions represent the projection of the 1×1 bulk band structure on the 2×1 SBZ.

$\bar{J}'_2$, and in addition, the energy position in the [110] azimuth, Fig. 3(a), is well above 0.5 eV at $\bar{J}'$. Thus, S_1 is not connected to the weak surface state band 0.7 eV below E_F at $\bar{J}'_2$. That feature, labeled S_d, will be discussed later in this paper.

In Fig. 3(a), a feature with very small dispersion is labeled S_2. This surface band is similar to a nearly dispersionless surface band reported in Ref. 9. Near $\bar{J}'(\bar{\Gamma}_2)$, it becomes less pronounced. Since it is not observed at $\bar{J}'_2$, S_2 is associated with the $\bar{\Gamma}$-$\bar{J}$-$\bar{\Gamma}_2$ direction in the SBZ.

A surface band that follows the $\bar{\Gamma}$-$\bar{J}'$ periodicity, is S_3. In Fig. 3(a), this surface state band appears to follow S_2 from $\bar{\Gamma}$ to $\bar{J}'/2$. In the outer part of the SBZ, it starts with a downward dispersion, followed by an upward dispersion, to finally reach 1.1 eV below E_F at the symmetry point $\bar{J}'$. A similar surface band, showing a downward dispersion in the outer part of the SBZ, was reported to reach about 1.3 eV below E_F near $\bar{J}'$ in Ref. 9. A discrepancy in the energy position might be explained by an unidentified surface feature, that was not observed in Ref. 9, which appears about 1 eV below E_F at $\bar{\Gamma}$ in Fig. 3. Due to surface umklapp, this feature can be expected to contribute at $\bar{\Gamma}_2$. This could introduce an uncertainty in the energy position of S_3 at $\bar{J}'$. Since S_3 is associated with the $\bar{\Gamma}$-$\bar{J}'$ direction, it is expected to show up at $\bar{J}'_2$ as well. A very weak dispersionless surface state band, labeled S_3, appears 1.3 eV below E_F near $\bar{J}'_2$ in Fig. 3(b). Based on the similarity with the band in Ref. 9 regarding the energy position at $\bar{J}'_2$ and with the uncertainty in energy position at $\bar{J}'$ in mind, this surface state band is believed to be the same S_3 as in Fig. 3(a).

The strongest surface state band in Fig. 3(b), is S_4. In the bulk band-gap region, a downward dispersion is easy to follow. As two surface state bands appear to merge at $\bar{k}_{\|} \sim 0.2$ Å^{-1}, it is difficult to determine whether S_4 belongs to the upper or to the lower branch at $\bar{\Gamma}$. At $\bar{J}'_2$, the energy position of S_4 is 2 eV below E_F. Surprisingly, it does not show up at all at this energy at $\bar{J}'$. An explanation to this will be discussed below, in connection with the calculated surface band structure.

About 3 eV below E_F, S_{bb} is found showing symmetry around $\bar{J}'_2$. As in the case of S_d, this surface state band is believed to be of different origin than S_1-S_4 and it will be discussed later in this paper. Here we note that none of the surface states show clear Rashba-type splitting in Fig. 3(a). This result indicates that the Rashba splitting is smaller than the experimental resolution in this system.

The two 2×1 models with 1 ML of Tl, which showed the lowest total energies in Ref. 4 were used in the calculations in this work. In Ref. 4, total energy calculations favored the pedestal+valley-bridge model, see Fig. 2(a). Showing a 0.23 eV higher total energy, the pedestal+cave model came in second place in that study. The cave site is located above a fourth layer Si atom in the trough, cf. the valley-bridge site which is above a third-layer Si atom. In our calculations the total energy difference between these two models came out as 0.25 eV. This indicates that the parameters used in our calculations, i.e., **k** mesh, energy cutoff, and slab geometry, produce results that are consistent with earlier work.

Figure 4 shows the calculated surface band structure, obtained using the model in Fig. 2(a). Simultaneous contributions from the two surface domains are shown by the overlapping black and gray surface bands in the [110] azimuth. Parts of four surface bands in the [110] and [010] directions are labeled Σ_1-Σ_4 and marked by solid circles. These bands describe the features in the ARPES data in Fig. 3. The atomic and orbital origins of the bands are summarized in Table I.

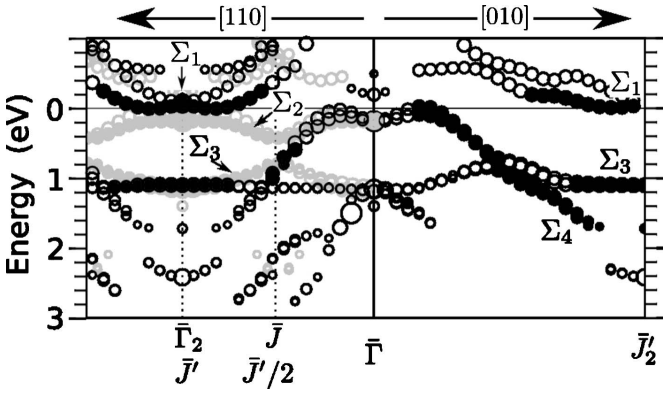

FIG. 4. Surface band dispersions calculated using the 1 ML Si(001):Tl 2×1 pedestal+valley-bridge model from Ref. 4. Large circles indicate strong surface character. Gray and black circles in the [110] azimuth illustrate the overlapping bands from the $\bar{\Gamma}$-$\bar{J}$-$\bar{\Gamma}$ and the $\bar{\Gamma}$-$\bar{J}'$ directions, respectively. Solid circles and the labels Σ_1-Σ_4, indicate the parts of the surface state bands that can describe features in the ARPES data. The orbital contributions to Σ_1-Σ_4 are summarized in Table I.

The large atomic mass of Tl (atomic number 81) motivates the inclusion of spin-orbit interaction in the calculations. A Rashba-type splitting, which was not observed experimentally, is clearly shown by Σ_1 at $\bar{J}'$ in the calculated surface band structure in Fig. 4. The Rashba parameter obtained from the calculation, α_R=0.44 eV Å, is larger than that obtained on Si(111):Tl (α_R=0.2 eV Å),[12] but smaller than on Si(111):Bi (α_R=1.37–2.3 eV Å).[13,14] This indicates that the combination of elements affects the Rashba splitting. Apart from splitting the bands, spin-orbit coupling gives rise to two very important changes in the surface band structure. First, spin-orbit effects shift Σ_1 down in energy by about 0.3 eV due to the strong contribution from Tl p orbitals. At this new energy position, it qualitatively describes the behavior of S_1. The second effect is the large (~5 eV) downshift of the Tl $6s^2$ states, i.e., the inert pair effect. The strongest individual contribution to the occupied surface bands comes from the Si dimer atoms. As a result of this, calculations performed with and without spin-orbit interaction included produce similar surface band dispersions, apart from the energy position of Σ_1.

In an STM study,[9] filled states were found to be localized at the position of Tl_1 while empty states were associated with Tl_2. The results in Table I are consistent with that study as Tl_1 is more strongly represented in the filled states while the relative contribution from Tl_2 is stronger for the empty, or partially empty, states.

An explanation for the missing S_4 at $\bar{J}'$ comes from considering the orbital contribution to the corresponding calculated band, Σ_4. As shown in Table I, this band has a strong contribution from the $p_{x'}$ orbitals of the Si dimer atoms, i.e., orbitals oriented along the Si dimer bond. This, in combination with the use of linearly polarized light in the ARPES study, can explain the fact the S_4 is not observed at $\bar{J}'$ in the [110] azimuth. The dimer bonds on the surface domain that is probed in the $\bar{\Gamma}$-$\bar{J}'$ direction in the [110] azimuth are oriented perpendicular to the polarization direction of the light. Therefore, electrons in these orbital can be expected to show a small excitation cross section.

TABLE I. Atomic and orbital origins of the surface bands in Fig. 4 and corresponding experimental surface state bands from the ARPES data in Fig. 3. Atomic labels and x', y', and z' directions correspond to those in Fig. 2(a).

Band	Major contribution (atom orbital)	ARPES feature
Σ_1	Tl_2-$\{p_{x'},p_{y'},p_{z'}\}$, Tl_1-$p_{x'}$	S_1
Σ_2	Tl_1-$p_{z'}$, Si-$p_{x'}$	S_2
Σ_3	Si-$p_{x'}$, Tl_1-$p_{x'}$, Si_2-$p_{z'}$	S_3
Σ_4	Si-$p_{x'}$	S_4

Two surface state bands in Fig. 3(b), S_d and S_{bb}, have no counterparts in the calculations. It is interesting to note that their relative energy positions and dispersions are very similar to those of the strong dangling bond and back-bond bands found on the clean Si(001) surface.[21] It is possible that they, or at least the back-bond like S_{bb}, have survived the structural changes imposed by the Tl adsorption. However, as they do not show up in the calculations and, in addition, are very weak it is perhaps more likely that they are related to areas with incomplete coverage.

IV. SUMMARY

Four surface state bands that are associated with the Tl induced reconstruction were found using ARPES. A comparison to calculations indicates that the pedestal+valley-bridge 2×1 model is a plausible atomic structure since the calculated surface band dispersions of Σ_1-Σ_4 in Fig. 4, show similar features as the experimentally observed surface states S_1-S_4 in Fig. 3. LEED patterns indicate the presence of a complicated mix of different higher order reconstructions at low temperature. The diffraction pattern shows some similarities to that of a $c(4\times6)$ periodicity, but, mixed with, e.g., spots indicating $\frac{1}{5}$ distances and $c(4\times8)$-like spots. The phase transition has no discernible effect on the surface band structure as data acquired at RT were very similar to those acquired at 100 K.

ACKNOWLEDGMENTS

This work was financially supported by the Swedish Research Council (VR). Parts of the calculations were performed on the Neolith cluster at the National Supercomputer Centre (NSC) in Linköping, Sweden.

[1] G. Lee, C. G. Hwang, N. D. Kim, J. Chung, J. S. Kim, and S. Lee, Phys. Rev. B **76**, 245409 (2007).
[2] V. G. Kotlyar, A. A. Saranin, A. V. Zotov, and T. V. Kasyanova, Surf. Sci. Lett. **543**, L663 (2003).
[3] K. Sakamoto, P. E. J. Eriksson, S. Mizuno, N. Ueno, H. Tochihara, and R. I. G. Uhrberg, Phys. Rev. B **74**, 075335 (2006).
[4] A. A. Saranin, A. V. Zotov, V. G. Kotlyar, I. A. Kuyanov, T. V. Kasyanova, A. Nishida, M. Kishida, Y. Murata, H. Okado, M. Katayama, and K. Oura, Phys. Rev. B **71**, 035312 (2005).
[5] T. Abukawa and S. Kono, Phys. Rev. B **37**, 9097 (1988).
[6] Y. Morikawa, K. Kobayashi, and K. Terakura, Surf. Sci. **283**, 377 (1993).
[7] A. A. Saranin, A. V. Zotov, I. A. Kuyanov, Yu. V. Luniakov, M. Katayama, and K. Oura, Phys. Rev. B **76**, 193302 (2007).
[8] A. A. Saranin, A. V. Zotov, M. Kishida, Y. Murata, S. Honda, M. Katayama, and K. Oura, Surf. Sci. **601**, 595 (2007).
[9] A. A. Saranin, A. V. Zotov, I. A. Kuyanov, V. G. Kotlyar, M. Kishida, Y. Murata, H. Okado, I. Matsuda, H. Morikawa, N. Miyata, S. Hasegawa, M. Katayama, and K. Oura, Phys. Rev. B **71**, 165307 (2005).
[10] A. Visikovskiy, S. Mizuno, and H. Tochihara, Phys. Rev. B **71**, 245407 (2005).
[11] E. I. Rashba, Sov. Phys. Solid State **2**, 1109 (1960).
[12] K. Sakamoto, T. Oda, A. Kimura, K. Miyamoto, M. Tsujikawa, A. Imai, N. Ueno, H. Namatame, M. Taniguchi, P. E. J. Eriksson, and R. I. G. Uhrberg, Phys. Rev. Lett. **102**, 096805 (2009).
[13] I. Gierz, T. Suzuki, E. Frantzeskakis, S. Pons, S. Ostanin, A. Ernst, J. Henk, M. Grioni, K. Kern, and C. R. Ast, Phys. Rev. Lett. **103**, 046803 (2009).
[14] K. Sakamoto, H. Kakuta, K. Sugawara, K. Miyamoto, A. Kimura, T. Kuzumaki, N. Ueno, E. Annese, J. Fujii, A. Kodama, T. Shishidou, H. Namatame, M. Taniguchi, T. Sato, T. Takahashi, and T. Oguchi, Phys. Rev. Lett. **103**, 156801 (2009).
[15] J. P. Perdew, K. Burke, and M. Ernzerhof, Phys. Rev. Lett. **77**, 3865 (1996).
[16] P. Blaha, K. Schwarz, G. K. H. Madsen, D. Kvasnicka, and J. Luitz, in *WIEN2K, An Augmented Plane Wave+Local Orbitals Program for Calculating Crystal Properties*, edited by Karlheinz Schwarz (Techical Universität, Wien, Austria, 2001).
[17] H. Ibach and H. Lüth, *Solid-State Physics: An Introduction to Principles of Materials Science*, 3rd ed. (Springer-Verlag, Berlin, 2003).
[18] A. Kokalj, Comp. Mater. Sci. **28**, 155 (2003).
[19] R. I. G. Uhrberg, R. D. Bringans, R. Z. Bacharach, and J. E. Northrup, J. Vac. Sci. Technol. A **4**, 1259 (1986).
[20] A. Savitzky and M. J. E. Golay, Anal. Chem. **36**, 1627 (1964).
[21] L. S. O. Johansson, R. I. G. Uhrberg, P. Mårtensson, and G. V. Hansson, Phys. Rev. B **42**, 1305 (1990).